



**HAL**  
open science

## **Soil concentrations and atmospheric emissions of biogenic hydrogen sulphide (H<sub>2</sub>S) in a Rhizophora mangrove forest**

Adrien Jacotot, Inès Gayral, Sarah Louise Robin, Cyril Marchand

### ► **To cite this version:**

Adrien Jacotot, Inès Gayral, Sarah Louise Robin, Cyril Marchand. Soil concentrations and atmospheric emissions of biogenic hydrogen sulphide (H<sub>2</sub>S) in a Rhizophora mangrove forest. *Estuarine, Coastal and Shelf Science*, 2023, 291, pp.108439. <10.1016/j.ecss.2023.108439>. <hal-04526181>

**HAL Id: hal-04526181**

**<https://hal.inrae.fr/hal-04526181v1>**

Submitted on 1 Oct 2025

HAL is a multi-disciplinary open access archive for the deposit and dissemination of scientific research documents, whether they are published or not. The documents may come from teaching and research institutions in France or abroad, or from public or private research centers.

L'archive ouverte pluridisciplinaire HAL, est destinée au dépôt et à la diffusion de documents scientifiques de niveau recherche, publiés ou non, émanant des établissements d'enseignement et de recherche français ou étrangers, des laboratoires publics ou privés.



Distributed under a Creative Commons CC BY-NC 4.0 - Attribution - Non-commercial use - International License

1 **Soil concentrations and atmospheric emissions of biogenic hydrogen sulphide (H<sub>2</sub>S) in a**  
2 ***Rhizophora* mangrove forest**

3

4 **Adrien Jacotot<sup>1,2\*</sup>, Inès Gayral<sup>2</sup>, Sarah Louise Robin<sup>2</sup>, Cyril Marchand<sup>2</sup>**

5 <sup>1</sup>Sol, Agro et hydrosystèmes, Spatialisation (SAS), UMR 1069, INRAE, Institut Agro, Rennes, France

6 <sup>2</sup>Université de la Nouvelle-Calédonie, ISEA, EA 7484, BPR4, 98851, Noumea, New Caledonia, France

7

8 \* Corresponding author at:

9 Sol, Agro et hydrosystèmes, Spatialisation (SAS), UMR 1069, INRAE, Institut Agro, Rennes, France

10 E-mail address: [adrien.jacotot1@gmail.com](mailto:adrien.jacotot1@gmail.com)

11

12 **Keywords: Mangrove, H<sub>2</sub>S fluxes, soil-gas concentration, diffusion gradient, Fick's law, New**  
13 **Caledonia**

14

15 **Abstract**

16 Mangrove forests are potentially large biogenic sources of atmospheric hydrogen sulphide  
17 (H<sub>2</sub>S), featuring among the carbon-richest ecosystems in the world associated with strong soil anoxia  
18 and large quantities of sulphates brought by tides. H<sub>2</sub>S is highly toxic and acts as a precursor for  
19 atmospheric sulphur compounds and sulphate aerosols, which contribute to acid deposition and  
20 have implications for global climate change. Therefore, understanding H<sub>2</sub>S emissions in mangroves  
21 holds great importance. Yet, its range of emissions remains uncertain. In this exploratory study, soil  
22 H<sub>2</sub>S concentrations were measured during tide stall at both high and low tide in a semi-arid  
23 mangrove, which has never been done before. Then, potential H<sub>2</sub>S fluxes to the atmosphere were  
24 estimated at low tide. Soil concentrations were greater at high tide than low tide, probably due to  
25 larger soil anoxia (average of -377 vs -179 mV), with average values of 1.40 ± 0.55 and

26  $0.73 \pm 0.32 \text{ mmol L}^{-1}$ , respectively. Temperature was a key factor controlling soil concentrations, with  
27 higher values in the warm season than in the cold season. Average  $\text{H}_2\text{S}$  emissions ranged from  
28  $5.81 \pm 2.58$  to  $28.74 \pm 6.98 \mu\text{g S m}^{-2} \text{ h}^{-1}$  with a mean value of  $14.90 \pm 7.90 \mu\text{g S m}^{-2} \text{ h}^{-1}$ . This study  
29 contributes to reducing the uncertainty in the variation range of  $\text{H}_2\text{S}$  fluxes from mangroves, which  
30 may be significant for the global sulphur cycle.

31

## 32 **1. Introduction**

33 Mangrove forests are ecosystems composed of C3 halophytic trees growing on the land-sea  
34 intertidal continuum on most (sub)tropical coasts of the world. Mangrove forests are renowned for  
35 their long-term carbon (C) sequestration potential, which has earned them a place on the “Blue  
36 Carbon” ecosystems list (Donato *et al.*, 2011). Their large C sequestration capacity stems from both  
37 i) large primary productivity of the trees and ii) oxygen-limited decomposition of soil organic matter  
38 (SOM) due to the almost permanently waterlogged conditions, in turn controlled by the local tidal  
39 regime. Aerobic oxidation of SOM, the energetically prevailing thermodynamic process, is mostly  
40 restricted to the topmost few centimetres of the soil and to micro-aerobic zones of the rhizosphere  
41 due to crab burrows and oxygen transfers from the atmosphere down to the soil (Kristensen *et al.*,  
42 2017). Dissimilatory sulphate reduction (DSR), a strictly anaerobic process, is the second dominant  
43 SOM decomposition pathway in mangrove soils, accounting for up to 50% of total C mineralization  
44 (Kristensen *et al.*, 2008). Hydrogen sulphide ( $\text{H}_2\text{S}$ ), produced by DSR (Barton *et al.*, 2014), is the main  
45 biogenic sulphur gas emitted from mangroves, contributing up to 70% of total S emissions (Ganguly  
46 *et al.*, 2018).  $\text{H}_2\text{S}$  is best known for its strong rotten egg odour and its high toxicity for animal and  
47 plant life (Barton *et al.*, 2014), but is also a precursor of atmospheric sulphur dioxide ( $\text{SO}_2$ ), sulphuric  
48 acid ( $\text{H}_2\text{SO}_4$ ) and sulphate ( $\text{SO}_4$ ) aerosols, which contribute to acid deposition. Additionally, sulphate  
49 aerosols impact global climate change, with a potential cooling effect of  $0.75 \text{ W m}^{-2}$  (Ganguly *et al.*,  
50 2018). According to Watts (2000),  $\text{H}_2\text{S}$  emissions from natural sources are larger than anthropogenic

51 emissions (4.42 vs 3.30 Tg yr<sup>-1</sup>). However, the contribution of coastal wetlands remains very  
52 uncertain, in particular that of mangrove forests due to a great scarcity of measurement data.  
53

## 54 **2. Material and methods**

55 In this context, the objectives of this work were to measure soil H<sub>2</sub>S concentrations and to  
56 estimate potential emissions to the atmosphere from a *Rhizophora* spp. mangrove forest in New  
57 Caledonia (Southern hemisphere; 22°16'49.3"S, 166°28'15.3"E). This mangrove ecosystem  
58 experiences a semi-diurnal tidal regime (range of 1.10 to 1.70 m), and a tropical wet and dry climate  
59 classified as category Aw according to the Köppen-Geiger classification. The region has two distinct  
60 seasons: a wet and warm season spanning from November to April, and a dry and cold one from  
61 May to October.

62 To measure porewater H<sub>2</sub>S concentrations in the soil, core samples were collected once per  
63 month between January and August 2017, during low and high tide. Triplicate porewater samples  
64 were extracted from six depths (-0.05 to -0.55 m with a 0.10 m interval) using Rhizon micro-samplers  
65 and transferred to gas-sealed vials with a nitrogen headspace (1:1 volume). Each vial was then  
66 shaken to achieve gas equilibrium between the dissolved sulfides in the porewater and the gas  
67 phase. Subsequently, a subsample of the vial headspace was taken for further analysis. Lastly, a  
68 supplementary gas sample was collected 5 cm above the soil during low tide to measure  
69 atmospheric H<sub>2</sub>S concentration. H<sub>2</sub>S concentrations were analysed using gas chromatography  
70 equipped with a pulsed flame photometric detector (PFPD, OI Analytical) for H<sub>2</sub>S detection  
71 (Shimadzu, GC-17A, Japan) and a GS-GasPro capillary column (30 m x 0.32 mm, Agilent Technologies,  
72 USA). Analytical conditions were set as follows: injector, oven, and detector temperatures were fixed  
73 at 200, 65 and 250 °C, respectively. Injection volume was 1 ml with a 1:20 split. Retention time for  
74 H<sub>2</sub>S was ~3.6 min. The peak areas were integrated and reported to a 7-points calibration curve  
75 created with pure nitrogen as zero and from dilutions of a 25 ppm H<sub>2</sub>S gas standard. The conversion

76 from partial pressure of H<sub>2</sub>S in the headspace (ppm) to concentration in the water samples (mmol L<sup>-1</sup>) were done following Bastviken *et al.* (2004), using Henry's law and a Henry's law constant of 0.1 M  
77 <sup>1</sup>) were done following Bastviken *et al.* (2004), using Henry's law and a Henry's law constant of 0.1 M  
78 atm<sup>-1</sup> (Sander, 1999).

79 In addition, an extra core was collected during six campaigns (January to June 2017) to measure  
80 redox potential, soil water content, pH, soil density, salinity and soil organic carbon content, both  
81 during low and high tide (Jacotot *et al.*, 2004).

82 H<sub>2</sub>S fluxes to the atmosphere were estimated for low-tide periods, when the soil is exposed to  
83 the atmosphere, using a soil-atmosphere gradient method (SAGM). The SAGM is based on Fick's first  
84 law that relates the gas concentration gradient between two depths with the gas diffusion  
85 coefficient in the soil (D<sub>s</sub>). The entire calculation procedure and the equations used are detailed in  
86 Supplementary Material. The use of SAGM is constrained by the determination of a proper value of  
87 the tortuosity factor ( $\epsilon$ ) that influences D<sub>s</sub>. This determination can be done *in-situ* using gas tracers,  
88 but also estimated using empirical models. Herein, five values of  $\epsilon$  were first determined with  
89 empirical models, all based on soil porosity and water content (Step 1 in Supplementary Material).  
90 To determine the optimal  $\epsilon$  value, we used a dataset from Jacotot *et al.* (2019) consisting of soil CH<sub>4</sub>  
91 concentrations, and surface to atmosphere CH<sub>4</sub> fluxes measured using incubation chambers. These  
92 measurements were obtained at the same site and on the same date as the H<sub>2</sub>S concentrations  
93 presented in this study. For detailed information regarding the measurement methodologies  
94 employed, please refer to Jacotot *et al.* (2019). Subsequently, the SAGM was applied to calculate five  
95 sets of CH<sub>4</sub> fluxes to the atmosphere using the five potentials values of  $\epsilon$  (Step 1). To assess the  
96 differences between the SAGM-derived CH<sub>4</sub> fluxes and the ones obtained from static chambers, the  
97 Normalized Root Mean Square Error (NRMSE) was calculated (Step 2 in Supplementary Material).  
98 Finally, the  $\epsilon$  value that yielded the lowest NRMSE was selected for the subsequent calculation of  
99 H<sub>2</sub>S fluxes by SAGM using measurements taken 0.05 m below and 0.05 m above the soil surface.

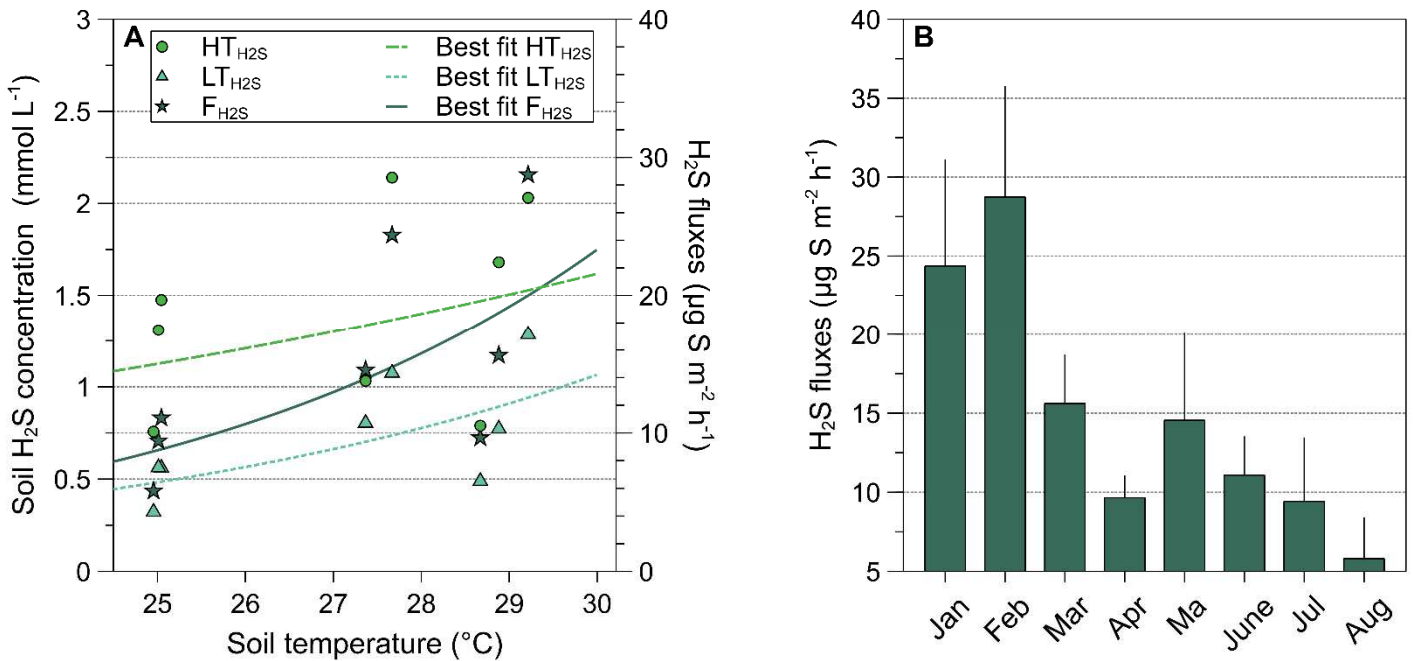
100

### 101 3. Results and discussion

102 Our results demonstrated that soil H<sub>2</sub>S concentrations varied over an order of magnitude  
103 and were driven by both tidal regime and seasonal temperature oscillations (Table 1 and Fig. 1A).  
104 Larger concentrations were observed at high tide ( $1.40 \pm 0.55$  mmol L<sup>-1</sup>, 0.34-2.40 mmol L<sup>-1</sup>) than at  
105 low tide ( $0.73 \pm 0.32$  mmol L<sup>-1</sup>, 0.16-1.44 mmol L<sup>-1</sup>). A possible hypothesis to explain the difference in  
106 concentrations between high and low tides is that during high tide, the waters from the lagoon  
107 circulating in the soil's interstitial pores may facilitate the renewal of electron acceptors by  
108 introducing sulphates. This, along with the strong anoxia of the sediment (redox values between -  
109 250 and -400 mV; Fig. 2A in Supplementary Material), could potentially support a high rate of DSR  
110 and accumulation of H<sub>2</sub>S. However, measurements of sulphate concentrations are necessary to  
111 support or reject this hypothesis. Conversely, at low tide the absence of a water column above the  
112 soil and a lower soil water content (Fig. 2E in Supplementary Material) allow i) emission of the H<sub>2</sub>S  
113 produced during high tide at the surface, and ii) oxygen diffusion within the soil, thus favouring  
114 aerobic SOM decomposition and H<sub>2</sub>S oxidation. In addition, whatever the tidal regime, seasonal  
115 differences in soil H<sub>2</sub>S concentrations were evidenced, with larger values during the warm season  
116 (Fig. 1A). While many factors can influence gas production, considering that all measurements were  
117 done during tide stall and that no significant variations in the physical and chemical drivers were  
118 observed between the warm and cool seasons except of temperature changes (see in Jacotot *et al.*,  
119 2019), we suggest that H<sub>2</sub>S soil concentrations were mainly driven by the seasonal temperature  
120 variability. Indeed, the temperature sensitivity of SOM decomposition is a phenomenon widely  
121 described in the literatures (*e.g.* Conant *et al.*, 2011; Davidson and Janssens, 2006). Eventually, no  
122 clear vertical stratification of H<sub>2</sub>S concentrations was observed, at either high or low tide, suggesting  
123 a relative homogeneity of the physical and chemical properties of the soil column that drive gas  
124 production and oxidation; which is supported by the low variability in depth of the physico-chemical  
125 parameters measured (Fig. 2 in Supplementary Material). Lastly, the concentrations measured in our  
126 study are comparable to those measured in the mangroves of Belize by Lee *et al.* (2008). However,

127 these authors observed a large increase in H<sub>2</sub>S concentrations below 15 cm depth, which was not  
 128 the case in our study. This difference may be attributed to the relative homogeneity of the soil  
 129 column, as discussed above.

130



132 Fig. 1: A) Relationships between A) Monthly averages of soil H<sub>2</sub>S concentrations and soil temperature  
 133 (°C), and B) Soil-atmosphere H<sub>2</sub>S fluxes (µg S m<sup>-2</sup> h<sup>-1</sup>) at low tide between January and August 2017.

134 In the left panel, circles and triangles indicate high tide (HT) and low tide (LT) soil concentrations,  
 135 respectively, while stars represent fluxes and lines are the best fit regressions with soil temperature.

136

137

138

139

140

141

142 Table 1: Soil H<sub>2</sub>S concentrations (mmol L<sup>-1</sup>) at low and high tide (mean ± SD) measured between

143 January and August 2017

Months (2017)	January	February	March	April	May	June	July	August
Depth (cm)	<i>High tide</i>							
5	2.40 ± 0.59	2.01 ± 0.39	1.70 ± 0.53	0.73 ± 0.30	1.54 ± 0.14	1.24 ± 0.77	0.76 ± 0.51	0.34 ± 0.30
15	2.34 ± 0.57	2.39 ± 0.71	2.03 ± 0.94	0.56 ± 0.09	1.19 ± 0.14	1.76 ± 0.49	1.16 ± 1.07	0.59 ± 0.52
25	2.02 ± 0.66	1.67 ± 0.31	1.97 ± 0.64	0.77 ± 0.16	0.74 ± 0.59	1.40 ± 0.07	1.42 ± 0.27	0.73 ± 0.47
35	2.10 ± 0.33	2.10 ± 0.67	1.26 ± 0.72	0.9 ± 0.14	0.87 ± 0.29	1.39 ± 0.10	1.60 ± 0.41	1.09 ± 0.50
45	1.77 ± 0.50	2.27 ± 1.14	1.65 ± 0.92	0.83 ± 0.17	0.83 ± 0.29	1.53 ± 0.07	1.35 ± 0.57	0.99 ± 0.92
55	2.20 ± 0.21	1.73 ± 0.59	1.47 ± 0.37	0.94 ± 0.03	1.02 ± 0.27	1.53 ± 0.14	1.58 ± 0.3	0.80 ± 0.50
Depth (cm)	<i>Low tide</i>							
5	1.21 ± 0.14	1.44 ± 0.74	0.73 ± 0.13	0.44 ± 0.04	0.87 ± 0.21	0.51 ± 0.09	0.30 ± 0.10	0.16 ± 0.07
15	1.22 ± 0.33	1.43 ± 0.34	0.77 ± 0.16	0.47 ± 0.07	0.71 ± 0.27	0.54 ± 0.11	0.47 ± 0.20	0.29 ± 0.13
25	0.94 ± 0.11	1.17 ± 0.11	0.83 ± 0.29	0.47 ± 0.03	0.92 ± 0.19	0.54 ± 0.04	0.59 ± 0.10	0.27 ± 0.07
35	1.13 ± 0.19	1.23 ± 0.13	0.73 ± 0.41	0.50 ± 0.04	1.00 ± 0.20	0.59 ± 0.07	0.63 ± 0.03	0.47 ± 0.07
45	0.94 ± 0.30	1.27 ± 0.49	0.67 ± 0.26	0.50 ± 0.06	0.57 ± 0.09	0.59 ± 0.10	0.62 ± 0.09	0.37 ± 0.09
55	1.00 ± 0.09	1.16 ± 0.19	0.90 ± 0.13	0.54 ± 0.06	0.74 ± 0.20	0.59 ± 0.10	0.77 ± 0.03	0.37 ± 0.11

144

145 At low tide, the estimated average soil-atmosphere H<sub>2</sub>S emission during the study period  
146 was 14.90 ± 7.90 μg S m<sup>-2</sup> h<sup>-1</sup> (Fig. 1B). The largest emissions were measured in February with  
147 28.74 ± 6.98 μg S m<sup>-2</sup> h<sup>-1</sup> and the smallest in August with 5.81 ± 2.58 μg S m<sup>-2</sup> h<sup>-1</sup>, consistent with the  
148 seasonal variation in soil H<sub>2</sub>S concentrations and temperature (Fig. 1A). However, it is possible that  
149 these fluxes are over-estimated. At low tide, mangrove soils are covered with a biological membrane  
150 composed of an assemblage of heterotrophic bacteria and autotrophic eukaryotes (Decho, 2000).  
151 This biofilm has been shown to act as a physical barrier, reducing gas transfer at the soil-air interface  
152 (see *e.g.* Jacotot *et al.*, 2019; Leopold *et al.*, 2013). In this study, theoretical fluxes were calculated

153 with the SAGM method, which does not account for a biofilm. As an indication, Jacotot *et al.* (2019)  
154 noted an average increase of ~17% in CH<sub>4</sub> fluxes after removing the biofilm. To put these numbers  
155 into perspective, we only found two studies of *in-situ* H<sub>2</sub>S fluxes in mangrove forests, and they both  
156 reported similar emissions to the present study, ranging from 3 to 31  $\mu\text{g S m}^{-2} \text{ h}^{-1}$  in Florida (Castro  
157 and Dierberg 1987), and from  $19 \pm 5$  to  $51 \pm 12$   $\mu\text{g S m}^{-2} \text{ h}^{-1}$  in the Sundarbans (Ganguly *et al.* 2018).  
158 By comparing these values to mangroves-associated ecosystems, such as saltmarshes, Delaune *et al.*  
159 (2002) reported H<sub>2</sub>S fluxes ranging from 5 to 79  $\mu\text{g S m}^{-2} \text{ h}^{-1}$ , which falls within the range of values  
160 observed in mangroves and and supports this range of emission values. Nevertheless, the available  
161 literature is currently insufficient to establish a plausible range of variation in H<sub>2</sub>S emissions from  
162 mangroves, as these may strongly differ in their physiographic characteristics. In addition, based on  
163 our study, extrapolating to an average H<sub>2</sub>S flux of the ecosystem is challenging because only low-tide  
164 fluxes were estimated. However, to estimate average fluxes, emissions based on the tidal cycle  
165 should be taken into account, as these ecosystems are submerged part of the time. Therefore, the  
166 presence of an oxygenated water column can potentially offset surface fluxes, as H<sub>2</sub>S can be oxidized  
167 during its diffusion. Regardless, based on an average from the available data for mangroves, the  
168 annual emissions would vary between 0.02 and 0.44  $\text{g S m}^{-2}$ , which, compared with the 0.035  $\text{g S m}^{-2}$   
169 reported by Yu *et al.* (2019) for coastal wetlands, would make mangroves potential hotspots of H<sub>2</sub>S  
170 emissions among coastal ecosystems.

171 In conclusion, this scoping study allowed for the determination of H<sub>2</sub>S fluxes in a semi-arid  
172 mangrove forest. The main important drivers of H<sub>2</sub>S emissions identified herein were the soil H<sub>2</sub>S  
173 concentrations as well as seasonal temperature variability. The fluxes presented here were similar to  
174 those reported by other studies, allowing further refining the global range of variation of H<sub>2</sub>S  
175 emissions from mangrove soils. A research effort should be performed to extend these measures to  
176 other mangrove sites that differ in their physiographical conditions, but also to understand the  
177 impact of local physicochemical parameters on H<sub>2</sub>S emissions.

178

179 **Acknowledgements**

180 This research was conducted as part of PhD thesis supported by the Province Sud of New  
181 Caledonia. We gratefully thank Chris R. Flechard, Scientist at the Institut National pour la Recherche  
182 en Agriculture, Alimentation et Environnement (INRAE) for his helpful comments on the manuscript.

183

184 **References**

- 185 Barton, L.L., Fardeau, M.-L., Fauque, G.D., 2014. Hydrogen Sulfide: A Toxic Gas Produced by  
186 Dissimilatory Sulfate and Sulfur Reduction and Consumed by Microbial Oxidation, in:  
187 Kroneck, P.M.H., Torres, M.E.S. (Eds.), *The Metal-Driven Biogeochemistry of Gaseous*  
188 *Compounds in the Environment, Metal Ions in Life Sciences*. Springer Netherlands,  
189 Dordrecht, pp. 237–277. [https://doi.org/10.1007/978-94-017-9269-1\\_10](https://doi.org/10.1007/978-94-017-9269-1_10)
- 190 Bastviken, D., Cole, J., Pace, M., Tranvik, L., 2004. Methane emissions from lakes: Dependence of  
191 lake characteristics, two regional assessments, and a global estimate: LAKE METHANE  
192 EMISSIONS. *Glob. Biogeochem. Cycles* 18, n/a-n/a. <https://doi.org/10.1029/2004GB002238>
- 193 Castro, M.S., Dierberg, F.E., 1987. Biogenic hydrogen sulfide emissions from selected Florida  
194 wetlands. *Water. Air. Soil Pollut.* 33, 1–13.
- 195 Conant, R.T., Ryan, M.G., Ågren, G.I., Birge, H.E., Davidson, E.A., Eliasson, P.E., Evans, S.E., Frey, S.D.,  
196 Giardina, C.P., Hopkins, F.M., Hyvönen, R., Kirschbaum, M.U.F., Lavallee, J.M., Leifeld, J.,  
197 Parton, W.J., Megan Steinweg, J., Wallenstein, M.D., Martin Wetterstedt, J. å., Bradford,  
198 M.A., 2011. Temperature and soil organic matter decomposition rates - synthesis of current  
199 knowledge and a way forward. *Glob. Change Biol.* 17, 3392–3404.  
200 <https://doi.org/10.1111/j.1365-2486.2011.02496.x>
- 201 Davidson, E.A., Janssens, I.A., 2006. Temperature sensitivity of soil carbon decomposition and  
202 feedbacks to climate change. *Nature* 440, 165–173. <https://doi.org/10.1038/nature04514>
- 203 Decho, A.W., 2000. Microbial biofilms in intertidal systems: an overview. *Cont. Shelf Res.* 17.
- 204 Delaune, R.D., Devai, I., Lindau, C.W., 2002. Flux of Reduced Sulfur Gases Along a Salinity Gradient in  
205 Louisiana Coastal Marshes. *Estuar. Coast. Shelf Sci.* 54, 1003–1011.  
206 <https://doi.org/10.1006/ecss.2001.0871>
- 207 Donato, D.C., Kauffman, J.B., Murdiyarto, D., Kurnianto, S., Stidham, M., Kanninen, M., 2011.  
208 Mangroves among the most carbon-rich forests in the tropics. *Nat. Geosci.* 4, 293–297.  
209 <https://doi.org/10.1038/ngeo1123>
- 210 Ganguly, D., Ray, R., Majumdar, N., Chowdhury, C., Jana, T.K., 2018. Biogenic hydrogen sulphide  
211 emissions and non-sea sulfate aerosols over the Indian Sundarban mangrove forest. *J.*  
212 *Atmospheric Chem.* 75, 319–333. <https://doi.org/10.1007/s10874-018-9382-3>
- 213 Jacotot, A., Marchand, C., Allenbach, M., 2019. Biofilm and temperature controls on greenhouse gas  
214 (CO<sub>2</sub> and CH<sub>4</sub>) emissions from a Rhizophora mangrove soil (New Caledonia). *Sci. Total*  
215 *Environ.* 650, 1019–1028. <https://doi.org/10.1016/j.scitotenv.2018.09.093>
- 216 Kristensen, E., Bouillon, S., Dittmar, T., Marchand, C., 2008. Organic carbon dynamics in mangrove  
217 ecosystems: A review. *Aquat. Bot.* 89, 201–219.  
218 <https://doi.org/10.1016/j.aquabot.2007.12.005>
- 219 Kristensen, E., Connolly, R.M., Otero, X.L., Marchand, C., Ferreira, T.O., Rivera-Monroy, V.H., 2017.  
220 *Biogeochemical Cycles: Global Approaches and Perspectives*, in: Rivera-Monroy, V.H., Lee,  
221 S.Y., Kristensen, E., Twilley, R.R. (Eds.), *Mangrove Ecosystems: A Global Biogeographic*

222 Perspective. Springer International Publishing, Cham, pp. 163–209.  
223 [https://doi.org/10.1007/978-3-319-62206-4\\_6](https://doi.org/10.1007/978-3-319-62206-4_6)  
224 Lee, R.Y., Porubsky, W.P., Feller, I.C., McKee, K.L., Joye, S.B., 2008. Porewater biogeochemistry and  
225 soil metabolism in dwarf red mangrove habitats (Twin Cays, Belize). *Biogeochemistry* 87,  
226 181–198. <https://doi.org/10.1007/s10533-008-9176-9>  
227 Leopold, A., Marchand, C., Deborde, J., Chaduteau, C., Allenbach, M., 2013. Influence of mangrove  
228 zonation on CO<sub>2</sub> fluxes at the sediment–air interface (New Caledonia). *Geoderma* 202–203,  
229 62–70. <https://doi.org/10.1016/j.geoderma.2013.03.008>  
230 Sander, R., 1999. Compilation of Henry’s Law Constants for Inorganic and Organic Species of  
231 Potential Importance in Environmental Chemistry (Version 3).  
232 Watts, S.F., 2000. The mass budgets of carbonyl sulfide, dimethyl sulfide, carbon disulfide and  
233 hydrogen sulfide. *Atmos. Environ.* 34, 761–779. [https://doi.org/10.1016/S1352-](https://doi.org/10.1016/S1352-2310(99)00342-8)  
234 [2310\(99\)00342-8](https://doi.org/10.1016/S1352-2310(99)00342-8)  
235 Yu, Q., Si, G., Zong, T., Mulder, J., Duan, L., 2019. High hydrogen sulfide emissions from subtropical  
236 forest soils based on field measurements in south China. *Sci. Total Environ.* 651, 1302–1309.  
237 <https://doi.org/10.1016/j.scitotenv.2018.09.301>  
238

